HOSTED BY

ELSEVIER

Available online at www.sciencedirect.com

ScienceDirect

Journal of Computational Design and Engineering 2 (2015) 113–118

www.elsevier.com/locate/jcde

An adaptive nonlocal filtering for low-dose CT in both image and projection domains

Yingmei Wang[a,1], Shujun Fu[a,*], Wanlong Li[b,1], Caiming Zhang[c,d]

[a]*School of Mathematics, Shandong University, Jinan, China*
[b]*Department of Radiation Oncology, Shandong Cancer Hospital and Institute, Jinan, China*
[c]*School of Computer Science and Technology, Shandong University of Finance and Economics, Jinan, China*
[d]*School of Computer Science and Technology, Shandong University, Jinan, China*

Received 25 November 2014; received in revised form 8 December 2014; accepted 12 December 2014
Available online 14 January 2015

Abstract

An important problem in low-dose CT is the image quality degradation caused by photon starvation. There are a lot of algorithms in sinogram domain or image domain to solve this problem. In view of strong self-similarity contained in the special sinusoid-like strip data in the sinogram space, we propose a novel non-local filtering, whose average weights are related to both the image FBP (filtered backprojection) reconstructed from restored sinogram data and the image directly FBP reconstructed from noisy sinogram data. In the process of sinogram restoration, we apply a non-local method with smoothness parameters adjusted adaptively to the variance of noisy sinogram data, which makes the method much effective for noise reduction in sinogram domain. Simulation experiments show that our proposed method by filtering in both image and projection domains has a better performance in noise reduction and details preservation in reconstructed images.

Keywords: Low-dose CT; Noise reduction; Sinogram restoration; Non-local filtering; Weighted average

1. Introduction

Computed tomography (CT) has gained extensive applications in medical and industrial fields. However, high-dose radiation increases the risk of cancer during the whole lifetime of patients and operators. In order to reduce radiation exposure caused by CT scanning, a simplest and most cost-effective way is to deliver fewer X-ray to an object or directly lower the tube current (mAs) as low as achievable in current CT systems. Consequently, the image quality with low-dose CT imaging will be severely degraded due to the photon starvation [1,2].

To get satisfactory reconstructed images for medical applications, the filtered backprojection (FBP) reconstruction algorithms based on projection restoration have been reported in previous researches [3–10]. There are also some direct image filtering algorithms in image domain [4,11,8], and mixed filtering methods in both domains [12].

Lu et al. did an experimental study on noise properties of X-ray CT sinogram data, and they found that the noise approximatively obeys a non-stationary Gaussian distribution [5]. Under this assumption, Cui et al. proposed a sinogram restoration method based on energy minimization in [10], which is a modified anisotropic diffusion with an adaptive smoothness parameter, where the algorithm performs well in both reducing noise and protecting the edge. However, there is still some obvious artifacts in the reconstructed images, and this is an iterative algorithm with low computational efficiency.

Although there have been lots of algorithms to deal with images with Gaussian noise in previous studies, fewer have not been used in CT images and sinogram data of low-dose CT simultaneously. Recently, the non-local means filtering was applied to medical image filtering for low-dose CT [7,11,12] since it was first proposed by Buades et al. [13] for natural image denoising.

*Corresponding author.
E-mail address: shujunfu@163.com (S. Fu).
[1]Both authors contributed equally to the paper.
Peer review under responsibility of Society of CAD/CAM Engineers.

http://dx.doi.org/10.1016/j.jcde.2014.12.007

Inspired by the idea of algorithms based on sinogram restoration such as the SR-NLM filtering [12], in order to deal with stripe artifacts in reconstructed image for low-dose CT, we develop a new adaptive nonlocal filtering for low-dose CT in both image and projection domains. In projection domain, its smoothness parameter is adjusted adaptively to the variance of noisy sinogram data; while in image domain, the smoothness parameter is adopted empirically, and the average weights are determined by the image FBP reconstructed from both the noisy sinogram and the non-local means restored sinogram. In following experiments it will be verified that our proposed approach has a better performance in noise reduction and details preservation in reconstructed images.

We organize the remaining part of this paper as follows. In Section 2, noise modeling and the main idea of the non-local means algorithm are presented, respectively, and then our proposed non-local means filtering based on sinogram restoration is described in detail. In Section 3, simulated experiments are implemented to verify the effectiveness and the feasibility of our proposed algorithm. In Section 4, we give the conclusion of this study.

2. Methods

2.1. Noise model

In this study, the calibrated and log-transformed projection data are called sinogram. The previous studies [3,5] have shown that low-dose sinogram data follow a non-stationary Gaussian distribution, with a non-linear relationship between the mean and the variance of the sinogram data, which is described by

$$\sigma_i^2 = f_i * \exp(p_i/\eta), \tag{1}$$

where p_i and σ_i denote the mean and standard deviation at detector bin i, respectively, while f_i and η are object-independent parameters that are specified by different CT systems. At the same time, it is shown that there are also some isolated points in extremely noisy regions of the sinogram data in [6].

2.2. Non-local means filtering

The non-local means (NLM) algorithm was first proposed by Buades et al. [13] for image denoising, which fully utilized the large redundancy of natural images and has been successfully applied to low-dose CT imaging [7,11,12]. Let Ω be a discrete grid of image pixels and $x = \{x_i | i \in \Omega\}$ be a noisy image, the denoised intensity $\mathrm{NLM}(x_i)$ at pixel i can be expressed by

$$\mathrm{NLM}(x_i) = \frac{\sum_{j \in \Omega} w(i,j) x_j}{\sum_{j \in \Omega} w(i,j)}, \tag{2}$$

where $w(i,j)$ is the average weight determined by the similarity between the pixels i and j, which is adopted as

$$w(i,j) = \exp\left\{ - \frac{\|x(N_i) - x(N_j)\|_{2,a}^2}{h^2} \right\}, \tag{3}$$

where N_i and N_j are similarity windows centered at pixels i and j, respectively; $\|\cdot\|_{2,a}$ denotes the Gaussian distance between two similarity windows with a standard deviation a; h denotes a smoothing factor that controls the decay of the exponential function in Eq. (3). To reduce the computational burden and improve the efficiency, the search window is always restricted to a proper local neighborhood S_i in Ω. The denominator of (2) is a normalizing factor.

2.3. Our method

The projection of a single point in any object forms a sinusoidal curve in the sinogram space. Because any object can be approximated by a collection of points located in space, its projection (sinogram) is obviously formed with a set of overlapped sine curves in the sinogram space [2]. As Buades et al. pointed that natural images have properties of sparsity and self-similarity in [13,14], sinogram data in low-dose CT are composed of special sinusoid-like strip data with same stronger self-similarity among these strip data (for example, see Fig. 2); FBP reconstructed images also have these properties, while noise does not have these special properties. So we can make use of this point to restore data contaminated seriously by noise. At the same time, we also find that we can match similar points more exactly by using the reconstructed image after sinogram restoration, which facilitates the aim of removing noise and preserving important details.

In the NLM algorithm, three parameters, i.e. search window, similarity window and smoothness parameter h, play an important role, among which h is especially critical. A larger h could cause too much smoothness in the data, while a smaller h would leave the restored data with excessive noise. In order to get a better weight in the NLM filtering, we develop our algorithm along two directions, including modifying the smoothness parameter h and the image intensity difference in similar neighborhoods. In this study, in order to find an appropriate h to smooth the data properly, ensuring the noise largely removed and the details preserved at the same time, we take two steps to adjust it both in the sinogram domain and in the image domain, respectively. In the following, we denote $p = \{p_k, k \in \Omega\}$ the low-dose CT sinogram data, $\tilde{p} = \{\tilde{p}_k, k \in \Omega\}$ the restored sinogram data by the NLM filtering, $I_{direct}^{FBP} = \{I_{direct,k}^{FBP}, k \in \Omega\}$ the image reconstructed from the noisy sinogram p, and $\tilde{I}_{sinoNLM}^{FBP} = \{I_{sinoNLM,k}^{FBP}, k \in \Omega\}$ the image reconstructed from the NLM filtered sinogram data $\tilde{p}$. Both I_{direct}^{FBP} and $\tilde{I}_{sinoNLM}^{FBP}$ are reconstructed by the FBP algorithm. As for the two steps to adjust the smoothness parameter h, firstly, in the sinogram domain we adjust $h = \{h_i, i \in \Omega\}$ to the standard deviation of the sinogram to control the smoothness of the NLM filtering

$$h_i = k_0 * \sigma_i, \tag{4}$$

where k_0 is a constant, σ_i is the standard deviation of the sinogram. The weight $w_{sino}(i,j)$ is then adopted as

$$w_{sino}(i,j) = \exp\left\{ - \frac{\|p(N_i) - p(N_j)\|_{2,a}^2}{h_i^2} \right\}, \tag{5}$$

where N_i and N_j are the similarity windows centered at pixels i and j, respectively. The term $p(N_i) := \{p_k, k \in N_i\}$ denotes the image intensity restricted in the similarity window N_i. And then the restored sinogram $\tilde{p}_i$ can be expressed by

$$\tilde{p}_i = \frac{\sum_{j \in N_i} w_{sino}(i,j) p_j}{\sum_{j \in N_j} w_{sino}(i,j)}. \tag{6}$$

Secondly, in the image domain, the smoothness parameter $\hat{h}$ is determined empirically. The weight $w_{img}(i,j)$ is determined by images I^{FBP}_{direct} and $\tilde{I}^{FBP}_{sinoNLM}$ to implement the NLM filtering in the image domain

$$w_{img}(i,j) = \exp\left\{ - \frac{\| I^{FBP}_{direct}(\overline{N}_i) - \tilde{I}^{FBP}_{sinoNLM}(\overline{N}_j) \|^2_{2,a}}{\hat{h}^2} \right\}, \tag{7}$$

where $\overline{N}_i$ and $\overline{N}_j$ are the similarity windows centered at pixels i, j in images I^{FBP}_{direct} and $\tilde{I}^{FBP}_{sinoNLM}$ respectively. $I^{FBP}_{direct}(\overline{N}_i) := \{I^{FBP}_{direct,k}, k \in \overline{N}_i\}$ denotes the image intensity restricted in the similarity window $\overline{N}_i$, and the term $\tilde{I}^{FBP}_{sinoNLM}(\overline{N}_j) := \{\tilde{I}^{FBP}_{sinoNLM,k}, k \in \overline{N}_j\}$ the image intensity restricted in the similarity window $\overline{N}_j$. Note that in (7) we take $I^{FBP}_{direct}(\overline{N}_i)$ and $\tilde{I}^{FBP}_{sinoNLM}(\overline{N}_j)$ other than just two similarity windows $\overline{N}_i$ and $\overline{N}_j$ of I^{FBP}_{direct} to determine the average weight. This is an effort that we make along the direction of modifying the image intensity difference in similar neighborhoods. From (7), we can see that the closer the noisy image I^{FBP}_{direct} is to the image $\tilde{I}^{FBP}_{sinoNLM}$, the larger the average weight is. Because the image $\tilde{I}^{FBP}_{sinoNLM}$ has been filtered a lot, it can be approximatively viewed as an exact image. That is to say, the closer the noisy image is to the exact image, the larger the average weight is, which makes the algorithm more effective to remove noise and preserve details.

Finally, we obtain the restored image $\hat{I} = \{\hat{I}_i, i \in \Omega\}$

$$\hat{I}_i = \frac{\sum_{j \in \hat{N}_i} w_{img}(i,j) I^{FBP}_{direct,j}}{\sum_{j \in \hat{N}_i} w_{img}(i,j)}, \tag{8}$$

where $\hat{N}_i$ denotes the search window centered at the pixel i in the reconstructed image I^{FBP}_{direct}.

As described above in (4), the smoothness parameter h_i in sinogram domain is adaptive to the noise variance σ_i of the sinogram, which will make the sinogram restoration algorithm more effective.

As for the isolated points in the noisy sinogram p, we use median filtering to filter them. For simplicity, we also denote the noisy sinogram with the isolated points removed as p, and then we summarize the procedure of our proposed NLM-based image restoration algorithm as follows in Fig. 1.

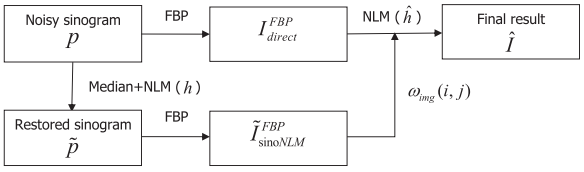

Fig. 1. Flow chart of our proposed algorithm.

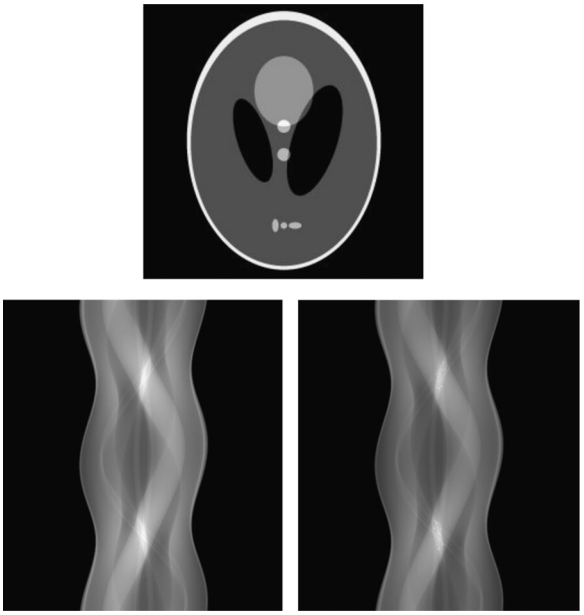

Fig. 2. 2-D Shepp–Logan head phantom and corresponding noise-free (bottom-left) and noisy (bottom-right) sinograms.

3. Simulations and results

We perform computer simulations to verify our method. The simulated sinogram data are produced by projecting the 2-D modified Shepp–Logan head phantom as shown in Fig. 2(a) using the fan-beam ray-driven algorithm. As described in [10], the size of sinogram is 888×984, where 888 and 984 are numbers of the detector bins and angle samples respectively. The noisy sinogram data for low-dose CT are simulated by adding isolated data and non-stationary Gaussian noise to the noise-free sinogram, where the variance of the non-stationary Gaussian noise is determined by the exponential relationship following formula (1). In this study we take $f_i = 100$, $\eta = 22{,}000$. The noise-free and noisy sinogram are shown in Fig. 2.

Firstly, the direct FBP (DFBP) reconstructed image from the noisy sinogram data, the reconstructed images by the FBP algorithm from the adaptive NLM filtered sinogram (SNLM), the energy minimization based anisotropic diffusion filtering (EMAD) [10], and the proposed algorithm (SINLM) are shown in Fig. 3, respectively. The results with different denoising methods are reconstructed by the standard FBP method using the Hanning filter.

For results by the DFBP and the SNLM methods, one can observe that there are severe noise-induced streak artifacts. The result by the EMAD method produces obviously annoying artifacts in some regions full of details. In contrast, there are hardly any streak artifacts in the result by our method. For a clear comparison, zoomed regions marked by the white rectangle boxes are shown in Fig. 4. One can observe that the EMAD method produces more streak artifacts than ours,

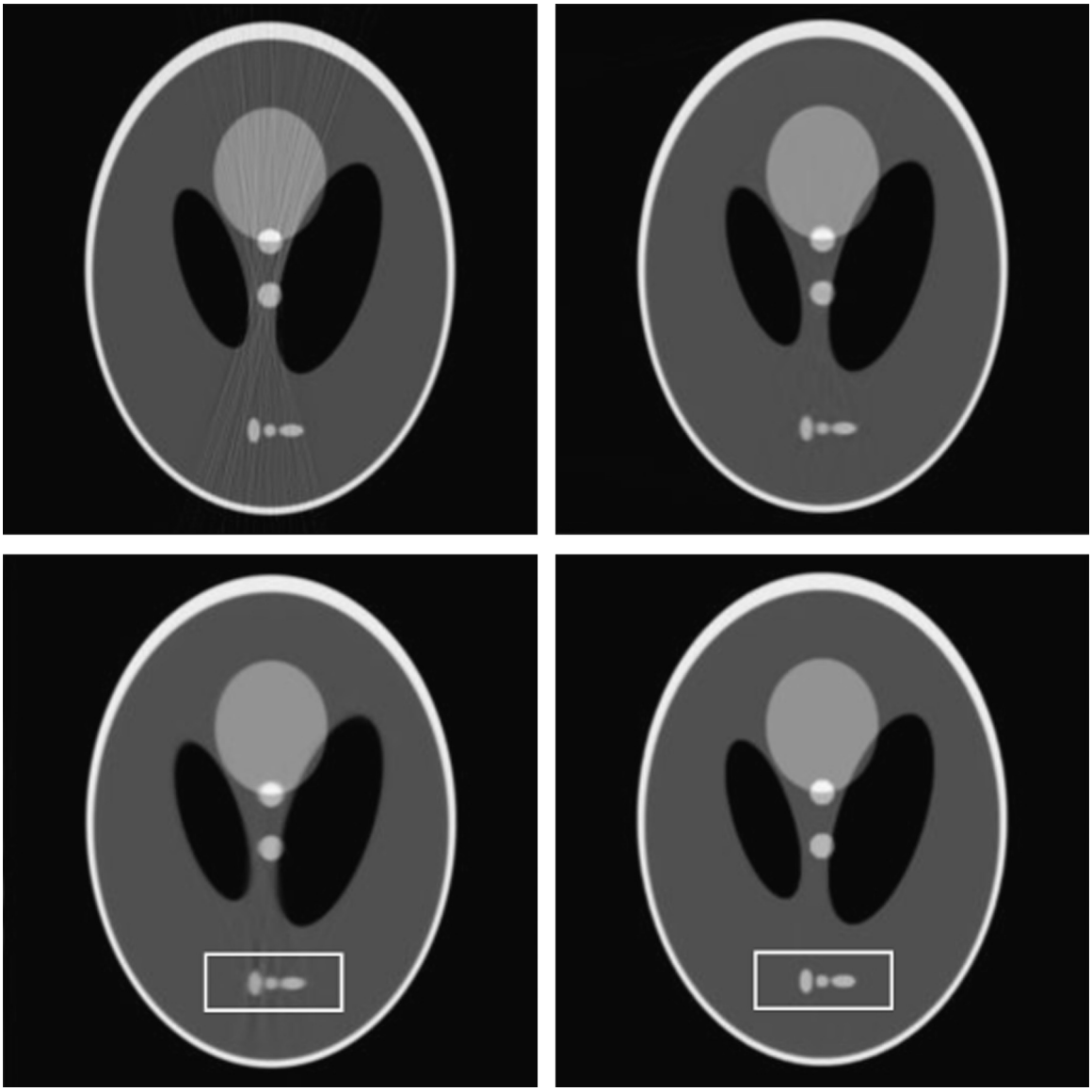

Fig. 3. Reconstructed images utilizing different methods (from top-left to bottom-right): DFBP, SNLM, EMAD, and SINLM. Regions marked by the white rectangle boxes are zoomed in for a clearer comparison in Fig. 4.

and our result is much closer than the EMAD's to the original image.

Secondly, to further illustrate the effectiveness of our proposed method, profiles along the 125th column of the reconstructed images by the EMAD and the SINLM methods, and its two zoomed parts are plotted in Fig. 5. One can observe that the profile of our result is much closer than the EMAD's to the profile of the original image. In smooth regions (marked by B), the profile curve of our result is much more smooth without apparent oscillation than the EMAD's, which implies that our method has a better performance in removing noise in smooth regions; as for image edges (marked by A), our result has bigger slope with a smaller width than the EMAD's, which means that our method can preserve the sharpness of edges and details much better.

Finally, we carry out quantitative comparisons to further validate our method. We calculate the signal to noise ratio

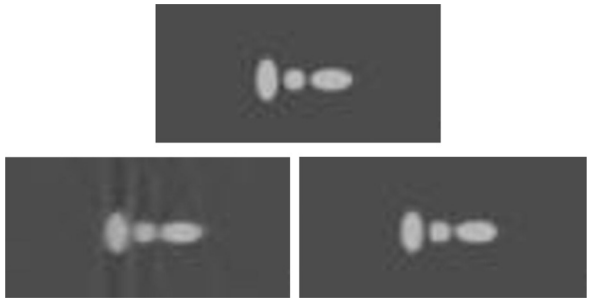

Fig. 4. Zoomed parts of images in Fig. 3 (from top to bottom-right): original simulation image, results by EMAD and SINLM.

(*SNR*) of the reconstructed images in Fig. 3, which is defined by

$$\mathrm{SNR} = -10\log_{10}\left(\int_{\Omega}(I-I_1)^2\,d\Omega \Big/ \int_{\Omega} I_1^2\,d\Omega\right). \tag{9}$$

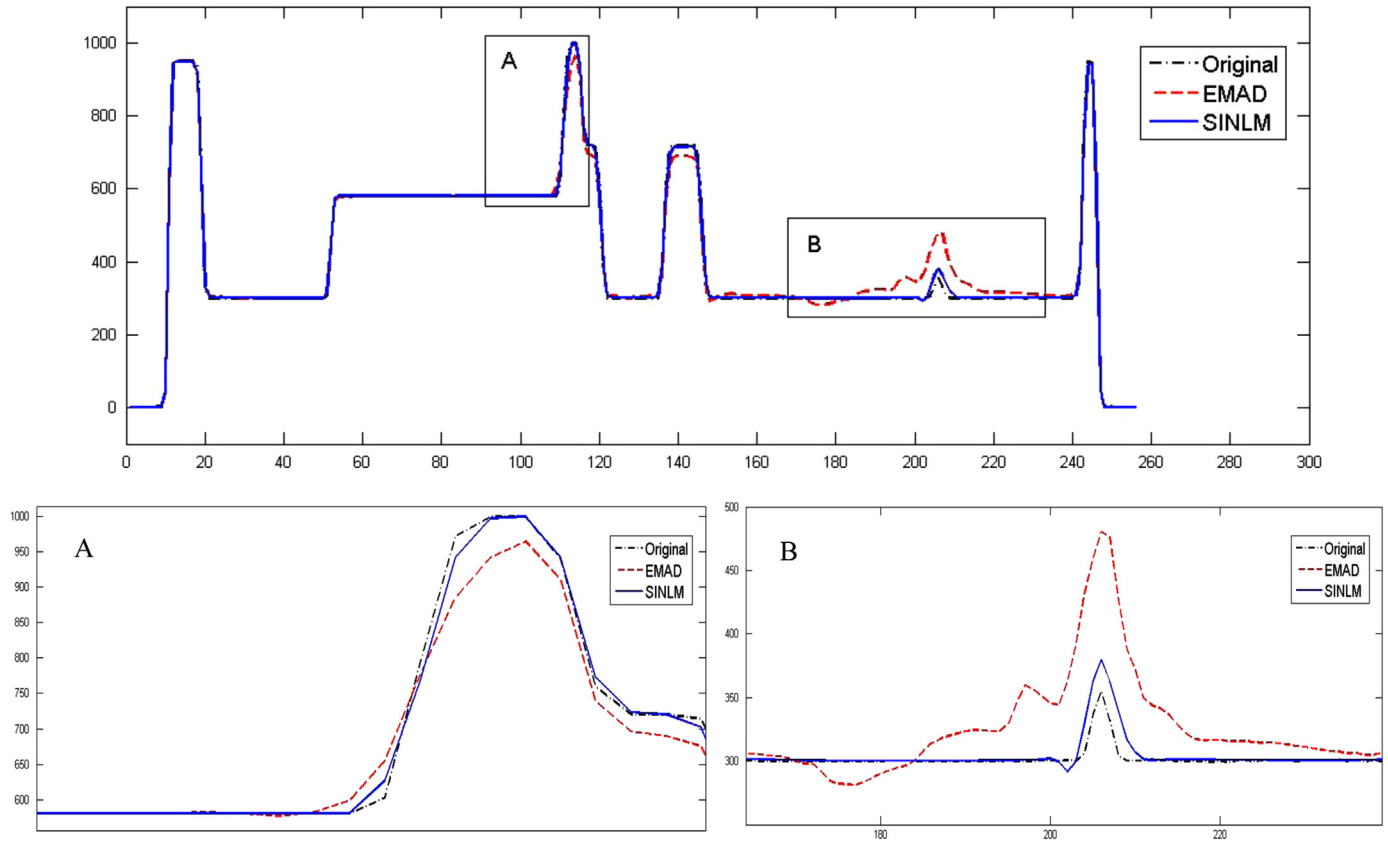

Fig. 5. Profiles along 125th column of reconstructed images by EMAD and SINLM, and two zoomed parts A and B.

In addition, we also calculate the normalized root mean square error (*NRMSE*) and the normalized mean absolute deviation (*NMAD*), which are formulated as follows:

$$\mathrm{NRMSE} = \sqrt{\int_{\Omega} (I - I_1)^2 / \sigma_1^2 \, d\Omega}, \tag{10}$$

$$\mathrm{NMAD} = \int_{\Omega} |I - I_1| / |I_1| \, d\Omega, \tag{11}$$

where σ_1 is the standard variance of the original image. The terms I and I_1 represent the reconstructed image and the original image, respectively. The index SNR reflects the noise level of an image, while the NRMSE and the NMAD imply the differences between the reconstructed image and the original image. The result of quantitative analysis is shown in Table 1, from which we can find that the image filtered with our proposed method has much higher SNR value and lower NRMSE and NMAD values than other images in Fig. 3. These results validate that our proposed method has the best quality.

In a word, from both the visual effects and the numerical indexes, our proposed algorithm performs much better than other methods in above experiments.

Table 1
SNR, *NMAD* and *NRMSE* results for low-dose reconstructed CT images by different methods.

	DFBP	EMAD	SNLM	SINLM
SNR	29.2288	30.4233	33.1803	34.0931
NMAD	0.1444	0.1275	0.1184	0.0985
NRMSE	0.0138	0.0126	0.0052	0.0054

4. Conclusions

In this paper, we develop a novel non-local filtering algorithm for low-dose CT based on the sinogram restoration. The proposed algorithm makes use of the advantage of self-similarity filtering to reduce the noise while preserving main details of important data. The experimental results show that the proposed method has better performance than some related restoration algorithms with respect to visual inspection and quantitative analysis. This is our first attempt at an effective low-dose CT imaging for properly reducing radiation damages in medical applications.

For future research, we will further try to optimize smoothness parameters in the process of non-local filtering according to the statistics of noise. At the same time, the techniques of speeding up the algorithm deserve deep research to approach to the proposed method.

Conflict of interest statement

The authors wishes to confirm that there are no known conflicts of interest associated with this publication and there

has been no significant financial support for this work that could have influenced its outcome.

Acknowledgments

The research has been partially supported by the National Natural Science Foundation of China (61272239, 61070094, and 61020106001), the NSFC Joint Fund with Guangdong (U1201258), the Science and Technology Development Project of Shandong Province of China (2014GGX101024), the Fundamental Research Funds of Shandong University (2014JC012), the Natural Science Foundation of Shandong province of China (ZR2011FM020), and the China Scholarship Council. We would like to thank Professor Zhiguo Gui of North University of China for his assistance on data simulation.

References

[1] Hsieh J. Adaptive streak artifact reduction in computed tomography resulting from excessive X-ray photon noise. *Medical Physics* 1998;**25**(11)2139–47.

[2] Hsieh Jiang. *Computed Tomography: Principles, Design, Artifacts, and Recent Advances*. Bellingham: SPIE; 2009.

[3] Li T, Li X, Wang J, Wen J, Lu H, Hsieh J, Liang Z. Nonlinear sinogram smoothing for low-dose X-ray CT. *IEEE Transactions on Nuclear Science* 2004;**51**(5)2505–13.

[4] Wang J, Li T, Lu H, Liang Z. Penalized weighted least-squares approach to sinogram noise reduction and image reconstruction for low-dose X-ray computed tomography. *IEEE Transactions on Medical Imaging* 2006;**25**(10)1272–83.

[5] Wang J, Lu H, Liang Z, Eremina D, Zhang G, Wang S, Chen J, Manzione J. An experimental study on the noise properties of X-ray CT sinogram data in Radon space. *Physics in Medicine and Biology* 2008;**53**(12)3327–41.

[6] Zhang Y, Zhang J, Lu H. Statistical sinogram smoothing for low-dose CT with segmentation based adaptive filtering. *IEEE Transactions on Nuclear Science* 2010;**57**(5)2587–98.

[7] Huang J, Ma J, Liu N, Feng Q, Chen W. Projection data restoration guided non-local means for low-dose computed tomography reconstruction. In: IEEE International Symposium on Biomedical Imaging; 2011; p. 1167–1170.

[8] Zhu Y, Zhao M, Zhao Y, Li H, Zhang P. Noise reduction with low dose CT data based on a modified ROF model. *Optics Express* 2012;**20**(16)17987–8004.

[9] Zhang Q, Gui Z, Chen Y, Li Y, Luo L. Bayesian sinogram smoothing with an anisotropic diffusion weighted prior for low-dose X-ray computed tomography. *Optik—International Journal for Light and Electron Optics* 2013;**124**(17)2811–6.

[10] Cui X, Zhang Q, Shangguan H, Liu Y, Gui Z. The adaptive sinogram restoration algorithm based on anisotropic diffusion by energy minimization for low-dose X-ray CT. *Optik—International Journal for Light and Electron Optics* 2014;**125**(5)1694–7.

[11] Ma J, Huang J, Feng Q, Zhang H, Lu H, Liang Z, Chen W. Low-dose computed tomography image restoration using previous normal-dose scan. *Medical Physics* 2011;**38**(10)5713–31.

[12] Bian Z, Ma J, Huang J, Zhang H, Niu S, Feng Q, Liang Z, Chen W. SR-NLM: *a sinogram restoration induced non-local means image filtering for low-dose computed tomography*. *Computerized Medical Imaging and Graphics* 2013;**37**(4)293–303.

[13] Buades A, Coll B, Morel JM. A review of image denoising algorithms, with a new one. *Multiscale Modeling and Simulation* 2005;**4**(2)490–530.

[14] Fu Shujun, Zhang Caiming. Fringe pattern denoising using averaging based on nonlocal self-similarity. *Optics Communications* 2012;**285**(10)2541–4.